# A Particular Bit of Universality: Scaling Limits of Some Dependent Percolation Models

Federico Camia[†]
Charles M. Newman[‡]
Vladas Sidoravicius[§]

March 10, 2004

**Abstract:** We study families of dependent site percolation models on the triangular lattice $\mathbb{T}$ and hexagonal lattice $\mathbb{H}$ that arise by applying certain cellular automata to independent percolation configurations. We analyze the scaling limit of such models and show that the distance between macroscopic portions of cluster boundaries of any two percolation models within one of our families goes to zero almost surely in the scaling limit. It follows that each of these cellular automaton generated dependent percolation models has the same scaling limit (in the sense of Aizenman-Burchard) as independent site percolation on $\mathbb{T}$.

*Keywords: continuum scaling limit, dependent percolation, universality, cellular automaton, zero-temperature dynamics*
*AMS Subject Classification: 82B27, 60K35, 82B43, 82C20, 82C43, 37B15, 68Q80*

[†]EURANDOM, P.O. Box 513, 5600 MB Eindhoven, The Netherlands
[‡]Courant Inst. of Mathematical Sciences, New York University, New York, NY 10012, USA
[§]Instituto de Matematica Pura e Aplicada, Rio de Janeiro, RJ, Brazil

# 1 Introduction

The phase diagrams of many physical systems have a "critical region" where all traditional approximation methods, such as mean-field theory and its generalizations, fail completely to provide an accurate description of the system's behavior. This is due to the existence of a "critical point," approaching which, some statistical-mechanical quantities diverge, while others stay finite but have divergent derivatives. Experimentally, it is found that these quantities usually behave in the critical region as a power law. The exponents that appear in those power laws, called **critical exponents**, describe the nature of the singularities at the critical point. The theory of critical phenomena based on the renormalization group suggests that statistical-mechanical systems fall into "universality classes" such that systems belonging to the same universality class have the same critical exponents.

It should be emphasized that the phenomenon of universality was discovered at least twice prior to the introduction of the renormalization group. In fact, in what Alan Sokal [50] calls the Dark Ages of the theory of critical phenomena, before the 1940's, physicists generally believed that all systems have the same critical exponents, namely those of the mean-field theory of Weiss [52] (1907) or its analogue for fluids, the van der Waals theory [51] (1873). The failure of this type of universality became apparent as early as 1900, following experiments on fluid systems, but it began to be taken seriously only after Onsager's exact solution [42] (explicitly displaying non-mean-field exponents) in 1944 and the rediscovery of the experimental evidence of non-mean-field values for critical exponents by Guggenheim in 1945 [24]. Nonetheless, although mean-field theory is clearly incorrect for short range models, some universality does seem to hold. Many, if not all, different fluids, for instance, seem to have the same value for the critical exponent $\beta$ (related to density fluctuations), and it is believed that, for example, carbon dioxide, xenon and the three dimensional Ising model should all have the same critical exponents. Maybe even more surprisingly, it was soon realized that some (but not all) magnetic systems have the same critical exponents as do the fluids. This remarkable phenomenon seems to suggest the existence of a mechanism that makes the details of the interaction irrelevant in the critical region. Nevertheless, the critical exponents should depend on the dimensionality of the system and on any symmetries in the Hamiltonian.

Despite being a very plausible and appealing heuristic idea, backed up by renormalization group arguments and empirical evidence, only very few cases are known in which some form of universality has actually been *proved*, especially below the *upper critical dimension*, where the values of the critical exponents are expected, and in some cases proved, to be different from those predicted by mean-field theory. There are, however, some more examples even in low dimensions – see, e.g., [8, 9, 11, 43]. In particular, in [8, 9] methods analogous to the ones developed here and in [11] are applied, but to different models and on different lattices.

Percolation, with its simplicity and important physical applications, is a natural candidate for studying universality. This is especially so after the ground-breaking work of Schramm [45], who identified the only possible conformally invariant scaling limit of critical percolation, and that of Smirnov [47, 48] (see also closely the related work of

Lawler, Schramm, and Werner [28, 29, 30, 31, 32, 33, 34]). The combination of those results made it possible [49] to verify the values of the critical exponents predicted in the physical literature in the case of critical site percolation on the triangular lattice (and to derive also some results that had not appeared in the physics literature, such as an analogue of Cardy's formula "in the bulk" [46], or the description of the so-called backbone exponent [32]).

It is generally accepted that the lattice should play no role in the scaling limit, and that there should be no difference between bond and site percolation. In other words, two-dimensional critical (independent) percolation models, both site and bond, should belong to the same universality class, regardless of the lattice (at least for periodic lattices like the square, triangular or hexagonal lattice). Once again, though, despite being a very natural and plausible conjecture, such universality has not yet been proved. There is however another natural direction in which to study universality, which consists in analyzing critical percolation models on a given lattice that differ in their dependence structures. It is this direction that we pursue in this paper.

The cellular automata that we use to generate our families of dependent percolation models arise naturally in the study of the zero-temperature limit of Glauber dynamics or as coarsening or agreement-inducing dynamics. The action of such cellular automata can be viewed as a sort of "small (local) perturbation" of the original, independent percolation model, and our main corollary can be viewed as proving a form of universality for two dimensional percolation. Therefore, we provide an explicit example of the principle of universality, in the strong form concerning scaling limits.

To be more precise, there are at least two, a priori different, notions of universality, one concerning the critical exponents discussed above, and a second one concerning the *continuum scaling limit*. The two concepts are closely related, but in this paper we are only concerned with the second type of universality. The first type is considered in [11], using methods related to, but easier than, those in this paper; it appears that universality in terms of the scaling limit is a stronger notion than that in terms of exponents. In [49], some knowledge of the scaling limit is used to determine critical exponents in the case of two-dimensional independent site percolation on the triangular lattice, but there is no general result in this direction.

We remark that the continuum limit used in this paper corresponds to the "full scaling limit" (for independent percolation) discussed in [12] (see also Theorem 4 and Subsection 3.3 of [47]). A complete proof of the existence and properties of the "full scaling limit" has, to our knowledge, not yet appeared in the literature, although there has been recent progress in that direction [12, 13].

We consider a family of dependent percolation models that arise through a (discrete time) deterministic cellular automaton T acting on site percolation configurations $\sigma$ on the set of sites of the triangular lattice $\mathbb{T}$. Each configuration $\sigma$ corresponds to an assignment of $-1$ or $+1$ to the vertices of $\mathbb{T}$. The variable $\sigma_x$, corresponding to the value of $\sigma$ at $x$, is commonly called a **spin** variable. At discrete times $n = 1, 2, \ldots$, each spin $\sigma_x$ is updated according to the following rules (later, in Section 4, we will introduce other cellular automata, both on $\mathbb{T}$ and $\mathbb{H}$, generated by different rules):

- if $x$ has three or more neighbors whose spin is the same as $\sigma_x$, then the latter does not change value,
- if $x$ has only two neighbors $y_1$ and $y_2$ that agree with $x$, *and* $y_1$ and $y_2$ are not neighbors, then $\sigma_x$ does not change value,
- otherwise, $\sigma_x$ changes value: $\sigma_x \to -\sigma_x$.

The starting configuration $\sigma^0$, at time $n = 0$, of our cellular automaton is chosen from a Bernoulli product measure corresponding to independent critical percolation, and the distributions at times $n \geq 1$ (including the final state as $n \to \infty$) of the discrete time deterministic dynamical process $\sigma^n$ are the other members of our family of dependent percolation models. We show that all those dependent percolation models have the same scaling limit, thus providing an explicit example in which universality can be proven. This comes as a corollary of our main result, Theorem 1. To explain the main result, we first need some terminology.

In the scaling limit, the *microscopic scale* of the system (i.e., the lattice spacing $\delta$) is sent to zero, while focus is kept on features manifested on a *macroscopic scale*. In the case of percolation, it is far from obvious how to describe such a limit and we only do so briefly here; for more details, see [1, 2, 3]. We will make use of the approach introduced by Aizenman and Burchard [3] (see also [4]) applied to portions of the boundaries between clusters of opposite sign, and present our results in terms of closed collections of curves in the one-point compactification $\dot{\mathbb{R}}^2$ of $\mathbb{R}^2$, which we identify (via the stereographic projection) with the two-dimensional unit sphere. For each fixed $\delta > 0$, the curves are, before compactification, polygonal paths of step size $\delta$ (i.e., polygonal paths between sites of dual lattice). The distance between curves is defined so that two curves are close if they shadow each other in a metric which shrinks at infinity (for the details, see Sections 2.2 and 2.3).

The dynamics allows one to construct the whole family of percolation models for all $n \in \{0, 1, \ldots, \infty\}$ on the same probability space, i.e., there is a natural coupling $\nu$, realized through the dynamics, between any two percolation models in the family. In terms of this coupling, Theorem 1 states, roughly speaking, that the $\nu$-probability that the distance between the two collections of curves corresponding to two distinct percolation models in the family is bounded away from zero vanishes as $\delta \to 0$. This means that, in the limit $\delta \to 0$, given any two models in the family, for every curve in one of them, there exists a curve in the other one that shadows the first curve and vice-versa.

The rest of the paper is organized as follows. In Section 2, we describe the behavior of the cellular automaton T, define the family of dependent percolation models dynamically generated by T, and state the main results. The proofs of the main results are contained in Section 3. The dynamics described in Section 2 is chosen as a prototypical example, but is not the only one for which our results apply. In Section 4, we introduce other such dynamics (both on $\mathbb{T}$ and $\mathbb{H}$), which can be obtained as suitable zero-temperature limits of stochastic Ising models.

# 2 Definitions and results

We start this section by giving a more detailed definition of one of the families of dependent percolation models that are the object of investigation of this paper. The models in that family are defined on the triangular lattice $\mathbb{T}$, embedded in $\mathbb{R}^2$ by identifying the sites of $\mathbb{T}$ with the elementary cells (i.e., regular hexagons) of the hexagonal (or honeycomb) lattice $\mathbb{H}$ (see Figure 1). We will use those models as a paradigm and will give for them explicit and detailed proofs of the results. Later on, we will point out how to modify the proofs to adapt them to the other models discussed in the paper.

In the rest of the paper, points of $\mathbb{R}^2$ will be denoted by $u$ and $v$, while for the sites of $\mathbb{T}$ we will use the Latin letters $x$, $y$, $z$ and the Greek letters $\zeta$ and $\xi$. An edge of $\mathbb{T}$ incident on sites $x$ and $y$ will be denoted by $\eta_{x,y}$, while by $\eta^*_{x,y}$ we denote the dual edge (in $\mathbb{H}$) perpendicular bisector of $\eta_{x,y}$.

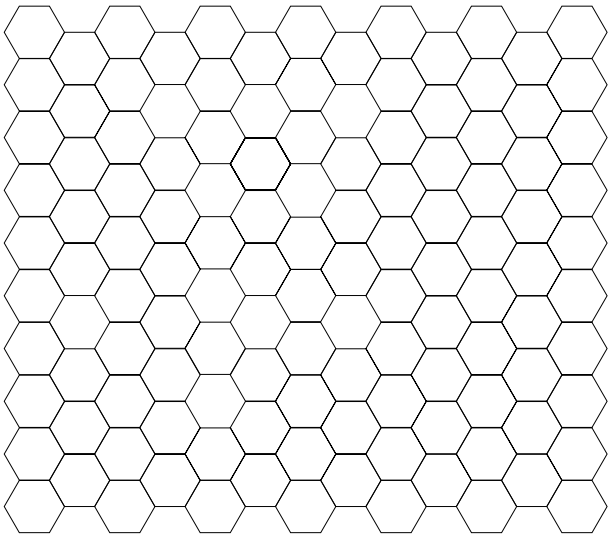

Figure 1: The hexagonal (or honeycomb) lattice.

## 2.1 The dynamics and the percolation models

We construct a family of dependent percolation models by means of a cellular automaton T acting on site percolation configurations on the triangular lattice $\mathbb{T}$, i.e., $\mathrm{T} : \Omega \to \Omega$, where $\Omega$ is the set of configurations $\{-1, +1\}^{\mathbb{T}}$. This family is parametrized by $n \in \{0, 1, \dots\} \cup \{\infty\}$ representing (discrete) time. The initial configuration $\sigma^0$ consists of an assignment of $-1$ or $+1$ to the sites of $\mathbb{T}$. At times, we will identify the spin variable $\sigma_x$ with the corresponding site (or hexagon) $x$. We choose $\sigma^0$ according to a probability measure $\mu^0$ corresponding to independent identically distributed $\sigma^0_x$'s with $\mu^0(\sigma^0_x = +1) = \lambda \in [0, 1]$. With the exception of Propositions 2.1 and 2.2, we will set $\lambda = 1/2$, so that $\mu^0$ is the distribution corresponding to critical independent site percolation. We denote by $\mu^n$ the

distribution of $\sigma^n$ and write $\mu^n = \tilde{\mathrm{T}}^n \mu^0$, where $\tilde{\mathrm{T}}$ is a map in the space of measures on $\Omega$. The action of the cellular automaton T can be described as follows:

$$\sigma_x^{n+1} = \begin{cases} \sigma_x^n & \text{if } x \text{ has at least two neighbors } y_1 \text{ and } y_2 \text{ such that } \sigma_{y_1}^n = \sigma_{y_2}^n = \sigma_x^n, \\ & \text{and } y_1 \text{ and } y_2 \text{ are not neighbors} \\ -\sigma_x^n & \text{otherwise} \end{cases} \tag{1}$$

Once the initial percolation configuration $\sigma^0$ is chosen, the dynamics is completely deterministic, that is, T is a deterministic cellular automaton with random initial state (see Figs. 2 and 3).

Certain configurations are stable for the dynamics, in other words, they are absorbing states for the cellular automaton. To see this, let us consider a loop in $\mathbb{T}$ expressed as a sequence of sites $(\zeta_0, \ldots, \zeta_k)$ which are distinct except that $\zeta_0 = \zeta_k$ and suppose moreover that $k \geq 6$ and that $\zeta_{i-1}$ and $\zeta_{i+1}$ are not neighbors; we will call such a sequence an **m-loop** (these are the "minimal" loops that can be "stable" – see Definitions 3.1 and 3.3). If $\sigma_{\zeta_0} = \sigma_{\zeta_1} = \ldots = \sigma_{\zeta_{k-1}}$ then every site $\zeta_i$ in such an m-loop has two neighbors, $\zeta_{i-1}$ and $\zeta_{i+1}$, such that $\zeta_{i-1}$ and $\zeta_{i+1}$ are not neighbors of each other and $\sigma_{\zeta_{i-1}} = \sigma_{\zeta_i} = \sigma_{\zeta_{i+1}}$. According to the rules of the dynamics, $\sigma_{\zeta_i}$ is therefore stable, that is, retains the same sign at all future times. Other stable configurations are "barbells," where a barbell consists of two disjoint such m-loops connected by a stable m-path. The stability of certain loops under the action of T will be a key ingredient in the proof of the main theorem. A more precise definition of m-paths and m-loops is given in Section 3.

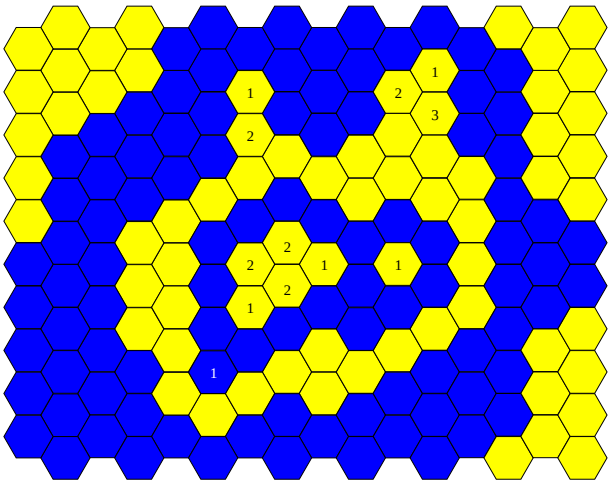


Figure 2: Example of local configuration with unstable spins. The numbered hexagons correspond to spins that will flip and the numbers indicate at what time step the spin flips occur.

An important feature of this dynamics is that almost surely every spin flips only a finite number of times and every local configuration gets fixated in finite time. To show this

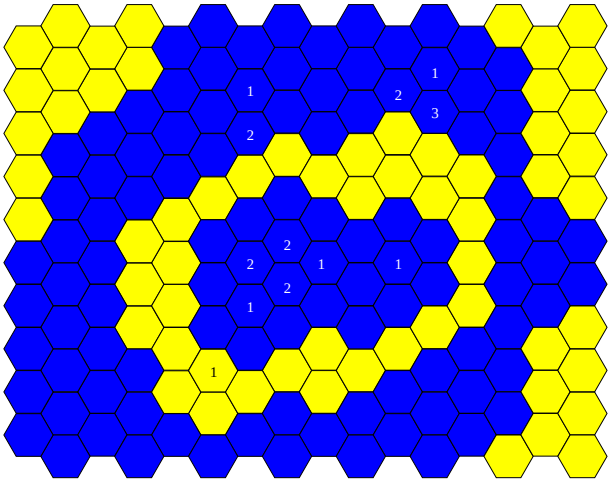

Figure 3: Same local configuration after all the unstable spins have flipped.

(and also to make more explicit the connection with the models discussed in Section 4), we introduce a formal Hamiltonian

$$\mathcal{H}(\sigma) = -\sum_{\langle x,y\rangle} \sigma_x \sigma_y = \frac{1}{2}\sum_x \mathcal{H}_x(\sigma), \tag{2}$$

where $\sum_{\langle x,y\rangle}$ denotes the sum over all pairs of neighbor sites, each pair counted once, and

$$\mathcal{H}_x(\sigma) = -\sum_{y\in\mathcal{N}(x)} \sigma_x \sigma_y, \tag{3}$$

where $\mathcal{N}(x)$ is the set of six (nearest) neighbors of $x$. We also introduce a "local energy"

$$\mathcal{H}_\Lambda(\sigma) = -\sum_{\substack{\langle x,y\rangle \\ x,y\in\Lambda}} \sigma_x \sigma_y - \sum_{z\in\partial\Lambda} \sum_{\substack{x\in\Lambda \\ x\in\mathcal{N}(z)}} \sigma_x \sigma_z, \tag{4}$$

where $\Lambda$ is a subset of $\mathbb{T}$ and $\partial\Lambda$ is the outer boundary of $\Lambda$, i.e., $\{\zeta \notin \Lambda : x \in \mathcal{N}(\zeta)$ for some $x \in \Lambda\}$. Notice that although the total energy $\mathcal{H}(\sigma)$ is almost surely infinite and is therefore only defined formally, we will only use local energies of finite subsets of $\mathbb{T}$.

The notion of the energy change caused by a spin flip is somewhat ambiguous in a cellular automaton because of the synchronous dynamics and hence multiple simultaneous spin flips. Nevertheless, it is easy to show (see the proof of Proposition 2.1) that each step of the dynamics either lowers or leaves unchanged the energy – both locally and globally. In this sense, our cellular automaton can be considered a zero-temperature dynamics (see, for example, [37] and references therein).

**Proposition 2.1.** *For all values of $\lambda$, almost surely, every spin flips only a finite number of times.*

*Proof.* By the translation invariance and ergodicity of the model, it is enough to prove the claim for the origin. At time zero, and for all values of $\lambda$, the origin is almost surely surrounded by an m-loop $\Gamma$ of spins of constant sign. (For $\lambda = 1/2$, there are infinitely many loops of both signs surrounding the origin.) Such an m-loop is stable for the dynamics and its spins retain the same sign at all times. Call $\Lambda$ the (a.s. finite) region surrounded by $\Gamma$. The energy $\mathcal{H}_\Lambda$ of the *finite* region $\Lambda$ is bounded below. Consequently, if we can show that no step of the dynamics ever raises $\mathcal{H}_\Lambda$, it would follow that there can only be a finite number of steps that strictly lower the energy $\mathcal{H}_\Lambda$.

Call an edge $\eta_{x,y}$ **satisfied** if $\sigma_x = \sigma_y$ and **unsatisfied** otherwise; then the change in energy $\mathcal{H}_\Lambda(\sigma^{n+1}) - \mathcal{H}_\Lambda(\sigma^n)$ is twice the difference between the number of satisfied edges at time $n$ that become unsatisfied at time $n+1$ and the number of unsatisfied edges at time $n$ that become satisfied at time $n+1$. The edges that change from satisfied to unsatisfied or vice-versa are those between spins that flip and their neighbors that do not, so

$$\mathcal{H}_\Lambda(\sigma^{n+1}) - \mathcal{H}_\Lambda(\sigma^n) = \sum_{x\in\Lambda\,:\,\sigma_x^{n+1}\neq\sigma_x^n} \sum_{y\in\mathcal{N}(x)} (\sigma_x^n\sigma_y^n - \sigma_x^{n+1}\sigma_y^{n+1}) = \sum_{x\in\Lambda\,:\,\sigma_x^{n+1}\neq\sigma_x^n} \Delta_n\mathcal{H}_x, \quad (5)$$

where

$$\Delta_n\mathcal{H}_x = \mathcal{H}_x(\sigma^{n+1}) - \mathcal{H}_x(\sigma^n). \quad (6)$$

Notice that the only nonzero contributions in the first sum of (5) come from those sites $y \in \Lambda$ that do not flip at time $n$. We want to show that $\Delta_n\mathcal{H}_x \leq 0$ for all $x \in \Lambda$ and find some $y$ with $\Delta_n\mathcal{H}_y < 0$ (assuming there was at least one spin flip inside $\Lambda$ at time $n$).

Call $D_x^n$ the number of disagreeing neighbors of $x$ at time $n$ and notice that a necessary condition for the spin at site $x$ to flip at that time is $D_x^n \geq 4$. Let us first consider the case $D_x^n \geq 5$ and assume, without loss of generality, that $\sigma_x^n = -1$ and $\sigma_x^{n+1} = +1$. Then, at time $n$, site $x$ has at least five plus-neighbors, and at least three of them have plus-spins at time $n+1$ (those having at time $n$ two plus-neighbors that are not neighbors of each other). This implies that the number of edges incident on $x$ that change from unsatisfied to satisfied is at least three, while the number of edges that change from satisfied to unsatisfied is one. Then,

$$\Delta_n\mathcal{H}_x = \sum_{y\in\mathcal{N}(x)} (\sigma_x^n\sigma_y^n - \sigma_x^{n+1}\sigma_y^{n+1}) < 0. \quad (7)$$

Next, we consider the case $D_x^n = 4$. Again, we can assume that $\sigma_x^n = -1 = -\sigma_x^{n+1}$. In this case, one can have two types of spin flips, one with $\mathcal{H}_x(\sigma^{n+1}) - \mathcal{H}_x(\sigma^n) < 0$ and one with $\mathcal{H}_x(\sigma^{n+1}) - \mathcal{H}_x(\sigma^n) = 0$. The second type occurs when, of the four neighbors of $x$ that are plus at time $n$, two remain plus at time $n+1$ (we call them $y_1$ and $y_2$) and the other two flip to minus (we call them $z_1$ and $z_2$), while the two neighbors that are minus at time $n$ remain minus at time $n+1$ (we call them $\tilde{y}_1$ and $\tilde{y}_2$). In this situation, site $x$ disagrees with four of its six neighbors both at time $n$ and at time $n+1$ (see Figure 4) and therefore $\mathcal{H}_x(\sigma^{n+1}) - \mathcal{H}_x(\sigma^n) = 0$.

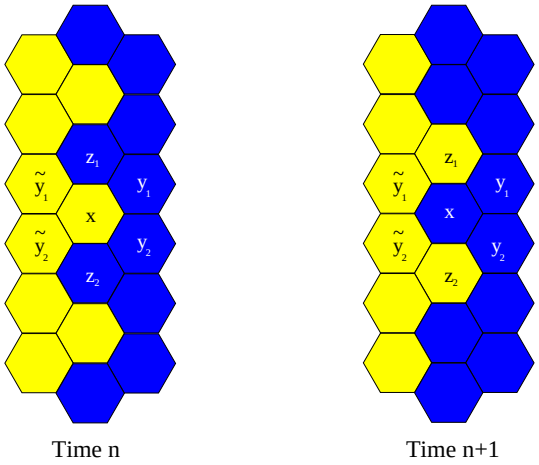


Figure 4: Example of a step of the dynamics acting on a local configuration that leaves the energy of some sites (including $x$) unchanged and decreases that of other sites (the three spins at the top and the three at the bottom are stable, as determined also by spins that do not appear in the figure).

The spins at $z_1$ and $z_2$ flip together with the spin at $x$. Each energy, $\mathcal{H}_{z_1}$ and $\mathcal{H}_{z_2}$, is lowered or left unchanged. If either is lowered, then the energy $\mathcal{H}_\Lambda$ is lowered. If neither is lowered, then $z_1$ and $z_2$ must be in the same situation as $x$ (but with minus and plus interchanged), which requires a configuration that looks locally like the one in the left part of Figure 4 (or one equivalent to it under some lattice symmetry). However, such a local configuration cannot extend forever; it must be finite and contained in $\Lambda$. This implies that we will necessarily find at least one spin $y$ (in fact, at least two spins) that flip together with the spin at $x$ and such that $\Delta_n \mathcal{H}_y < 0$.

Thus, if at time $n$ some site $x \in \Lambda$ flips,

$$\mathcal{H}_\Lambda(\sigma^{n+1}) - \mathcal{H}_\Lambda(\sigma^n) = \sum_{x \in \Lambda \,:\, \sigma_x^{n+1} \neq \sigma_x^n} \Delta_n \mathcal{H}_x < 0. \tag{8}$$

It follows that there can only be a finite number of times $n$ at which spins in $\Lambda$ (in particular, the origin) flip. This completes the proof. □

Let us now give two results that are analogous to results proved in [14] for a related cellular automaton that will be discussed below in Section 4.

**Proposition 2.2.** *If $\lambda > 1/2$ (respectively, $< 1/2$), then for almost every $\sigma^0$, there is percolation of $+1$ (respectively, $-1$) spins in $\sigma^n$ for any $n \in [0, \infty]$.*

*Proof.* We only give the proof for $\lambda > 1/2$, since the case $\lambda < 1/2$ is the same by symmetry. If $\lambda > 1/2$, since the critical value for independent (Bernoulli) percolation on the triangular lattice is exactly $1/2$, there is at time zero percolation of $+1$ spins. This implies

the existence, at time 0, of doubly-infinite plus-paths (i.e., plus-paths that can be split into two disjoint infinite paths) that are stable. Therefore, there is percolation of $+1$ spins for all $n \geq 0$. □

We denote by $C_x$ the cluster at $x$ (for a configuration $\sigma$), i.e., the maximal connected set $B \in \mathbb{T}$ such that $x \in B$ and $\sigma_y = \sigma_x$ for all $y \in B$. We write $C_x(n)$ to indicate the cluster at $x$ for $\sigma^n$. $C_x(n)$ is random and its distribution is denoted $\mu^n$. $\mathrm{E}_{\mu^n}$ denotes expectation with respect to $\mu^n$.

**Proposition 2.3.** *For $\lambda = 1/2$, the following two properties are valid.*

1. *For almost every $\sigma^0$, there is no percolation in $\sigma^n$ of either $+1$ or $-1$ spins for any $n \in [0, \infty]$.*
2. *The mean cluster size in $\sigma^n$ is infinite for any $n \in [0, \infty]$ : for any $x \in \mathbb{T}$,*

$$\mathrm{E}_{\mu^n}(|C_x|) = \mathrm{E}_{\mu^0}(|C_x(n)|) = \infty. \tag{9}$$

*Proof.* To prove the first claim, notice that at time zero the origin is almost surely surrounded by both a plus and a minus m-loop. Those loops are stable and prevent the cluster at the origin, be it a plus or a minus cluster, from percolating at all subsequent times. Therefore the probability that the origin belongs to an infinite cluster is zero for all $n \geq 0$.

To prove the second claim, we note that because of the absence of percolation for either sign, it follows from a theorem of Russo [44] applied to the triangular lattice, that the mean cluster size of both plus and minus clusters diverges. □

Before stating our main theorem, we need some more definitions to formulate the continuum scaling limit. We adopt the approach of [3] (see also [4]).

## 2.2 Compactification of $\mathbb{R}^2$

The scaling limit $\delta \to 0$ can be taken by focusing on fixed finite regions, $\Lambda \subset \mathbb{R}^2$, or by treating the whole $\mathbb{R}^2$. The second option is more convenient, because it avoids technical issues that arise near the boundary of $\Lambda$.

A convenient way of dealing with the whole $\mathbb{R}^2$ is to replace the Euclidean metric with a distance function $\mathrm{d}(\cdot, \cdot)$ defined on $\mathbb{R}^2 \times \mathbb{R}^2$ by

$$\mathrm{d}(u, v) = \inf_{\phi} \int (1 + |\phi|^2)^{-1} \, ds, \tag{10}$$

where the infimum is over all smooth curves $\phi(s)$ joining $u$ with $v$, parametrized by arc-length $s$, and $|\cdot|$ denotes the Euclidean norm. This metric is equivalent to the Euclidean metric in bounded regions, but it has the advantage of making $\mathbb{R}^2$ precompact. Adding a single point at infinity yields the compact space $\dot{\mathbb{R}}^2$ which is isometric, via stereographic projection, to the two-dimensional sphere.

## 2.3 The space of curves

Denote by $\mathcal{S}$ the complete, separable metric space of continuous curves in $\dot{\mathbb{R}}^2$ with a distance $\mathrm{D}(\cdot,\cdot)$ based on the metric defined by eq. (10) as follows. Curves are regarded as equivalence classes of continuous functions $\gamma(t)$ from the unit interval to $\dot{\mathbb{R}}^2$, modulo monotonic reparametrizations. $\mathcal{C}$ will represent a particular curve and $\gamma(t), t \in [0,1]$, a particular parametrization of $\mathcal{C}$, while $\mathcal{F}$ will represent a set of curves. The distance D between two curves, $\mathcal{C}_1$ and $\mathcal{C}_2$, is defined by

$$\mathrm{D}(\mathcal{C}_1,\mathcal{C}_2) \equiv \inf_{f_1,f_2} \sup_{t\in[0,1]} \mathrm{d}(\gamma_1(f_1(t)),\gamma_2(f_2(t))), \tag{11}$$

where $\gamma_1$ and $\gamma_2$ are particular parametrizations of $\mathcal{C}_1$ and $\mathcal{C}_2$, and the infimum is over the set of all monotone (increasing or decreasing) continuous functions from the unit interval onto itself. The distance between two closed sets of curves is defined by the induced Hausdorff metric as follows:

$$\mathrm{dist}(\mathcal{F},\mathcal{F}') \le \varepsilon \Leftrightarrow \forall\, \mathcal{C} \in \mathcal{F},\ \exists\, \mathcal{C}' \in \mathcal{F}' \text{ with } \mathrm{D}(\mathcal{C},\mathcal{C}') \le \varepsilon, \text{ and vice-versa.} \tag{12}$$

For each fixed $\delta > 0$, the random curves that we consider are polygonal paths in the hexagonal lattice $\delta\mathbb{H}$, dual of $\delta\mathbb{T}$, consisting of connected portions of the boundaries between plus and minus clusters in $\delta\mathbb{T}$. A subscript $\delta$ may then be added to indicate that the curves correspond to a model with a "short distance cutoff." The probability measure $\mu_\delta^n$ denotes the distribution of the random set of curves $\mathcal{F}_\delta^n$ consisting of the polygonal paths on $\delta\mathbb{H}$ generated by $\mathrm{T}^n$ acting on $\sigma^0$.

## 2.4 Main results

Since the cellular automaton is deterministic, all the percolation models $\sigma^n$ for $n \ge 0$ are automatically coupled, once they are all constructed on the single probability space $(\Omega,\Sigma,\mu^0)$ on which $\sigma^0$ is defined. The following theorem is valid for any $\lambda$, but $\lambda = 1/2$ is the only interesting case, therefore we restrict attention to it.

**Theorem 1.** *For $\lambda = 1/2$, the Hausdorff distance between the system of random curves $\mathcal{F}_\delta^0$ at time 0 and the corresponding system of curves $\mathcal{F}_\delta^n$ at time $n$ goes to zero almost surely as $\delta \to 0$, for each $n \in [1,\infty]$; i.e., for $\mu^0$-almost every $\sigma^0$,*

$$\lim_{\delta\to 0} \mathrm{dist}(\mathcal{F}_\delta^0,\mathcal{F}_\delta^n) = 0, \ \textit{for any } n \in [1,\infty]. \tag{13}$$

The main application of the theorem is that the scaling limits of our family $\mathcal{F}_1^n$ of percolation models, if they exist, must be the same for all $n \in [0,\infty]$:

**Corollary 2.1.** *Suppose that critical site percolation on the triangular lattice has a unique scaling limit in the Aizenman-Burchard sense [3], i.e., $\mathcal{F}_\delta^0$ converges in distribution as $\delta \to 0$ (for $\lambda = 1/2$). Then, for every $n \in [1,\infty]$, $\mathcal{F}_\delta^n$ converges in distribution to the same limit.*

**Remark 2.1.** *A complete proof of the convergence in distribution of $\mathcal{F}_\delta^0$ as $\delta \to 0$ (i.e., of the existence of the "full scaling limit" of independent site percolation on the triangular lattice as discussed in [47, 12]) has not yet appeared in the literature. A paper by two of the authors with a proof of this fact and of other properties of the limit, starting from Smirnov's results [48], is in preparation [13]. We also note that the proofs below show that the convergence in Theorem 1 and Corollary 2.1 is uniform in $n$.*

# 3 Proofs

In this section, we give the proofs of the main results. We start by reminding the reader of the definitions of m-path and m-loop and by giving some new definitions and two lemmas which will be used later.

**Definition 3.1.** *A* **path** $\Gamma$ *between $x$ and $y$ in $\delta\mathbb{T}$ (embedded in $\mathbb{R}^2$) is an ordered sequence of sites $(\zeta_0 = x, \ldots, \zeta_k = y)$ with $\zeta_i \neq \zeta_j$ for $i \neq j$ and $\zeta_{i+1} \in \mathcal{N}(\zeta_i)$. A* **loop** *is a sequence $(\zeta_0, \ldots, \zeta_{k+1} = \zeta_0)$ with $k \geq 1$ such that $(\zeta_0, \ldots, \zeta_k)$ and $(\zeta_1, \ldots, \zeta_{k+1})$ are paths.*

*We call a path $(\zeta_0, \ldots, \zeta_k)$ (resp., a loop $(\zeta_0, \ldots, \zeta_{k+1} = \zeta_0)$) an* **m-path** *(resp., an* **m-loop***) if $\zeta_{i-1}$ and $\zeta_{i+1}$ are not neighbors for $i = 1, \ldots, k-1$ (resp., for $i = 1, \ldots, k+1$, where $\zeta_{k+2} = \zeta_1$).*

Notice that for every path $\Gamma$ between $x$ and $y$, there always exists at least one m-path $\tilde{\Gamma}$ between the same sites.

**Definition 3.2.** *A* **boundary path** *(***b-path***) $\Gamma^*$ is an ordered sequence of distinct dual edges $(\eta_0^* = \eta_{\zeta_0,\xi_0}^*, \ldots, \eta_k^* = \eta_{\zeta_k,\xi_k}^*)$ such that either $\zeta_{i+1} = \zeta_i$ and $\xi_{i+1} \in \mathcal{N}(\xi_i)$ or $\xi_{i+1} = \xi_i$ and $\zeta_{i+1} \in \mathcal{N}(\zeta_i)$, and $\sigma_{\zeta_i} = -\sigma_{\xi_i}$ for all $i = 0, \ldots, k$.*

*We call a maximal boundary path simply a* **boundary***; it can either be a doubly-infinite path or a finite loop.*

b-paths represent the (random) curves introduced in the previous section for a fixed value of the short distance cutoff $\delta$. A collection of such curves in the compact space $\dot{\mathbb{R}}^2$ is indicated by $\mathcal{F}_\delta$.

b-paths $\Gamma^*$ are parametrized by functions $\gamma(t)$, with $t \in [0, 1]$. When we write that, for $t$ in some interval $[t_1, t_2]$ (the interval could as well be open or half-open), $\gamma(t) \in \eta_{x,y}^*$ we mean that the parametrization $\gamma(t)$ for $t$ between $t_1$ and $t_2$ is irrelevant and can be chosen, for example, so that $|\frac{d\gamma(t)}{dt}|$ is constant for $t \in [t_1, t_2]$. The notation $\Gamma^*(u, v)$, where $u$ and $v$ can be dual sites or generic points of $\mathbb{R}^2 \cap \Gamma^*$, stands for the portion of $\Gamma^*$ between $u$ and $v$.

**Definition 3.3.** *A* **stable loop** *$l$ (for some $\sigma$) is an m-loop $(\zeta_0 = x, \ldots, \zeta_k = x)$ such that $\sigma_{\zeta_0} = \sigma_{\zeta_1} = \ldots = \sigma_{\zeta_k}$.*

**Definition 3.4.** *We say that a dual edge $\eta_{x,y}^*$ is* **stable** *if $x$ and $y$ belong to stable loops of opposite sign.*

**Lemma 3.1.** *In general, a constant sign m-path $(\zeta_0, \ldots, \zeta_k)$ is "fixated" (i.e., retains that same sign in $\sigma^n$ for all $0 \leq n \leq \infty$) if $\zeta_0$ and $\zeta_k$ are fixated*

*Proof.* The claim of the lemma is straightforward.

**Lemma 3.2.** *For $\lambda = 1/2$, there is a one to one mapping from boundaries in $\mathcal{F}_\delta^{n+1}$ to "parent" boundaries in $\mathcal{F}_\delta^n$.*

*Proof.* Let $\Gamma_n^* \in \mathcal{F}_\delta^n$ be a boundary at time $n$ and $\mathrm{int}(\Gamma_n^*)$ be the set of sites of $\mathbb{T}$ (i.e., hexagons) "surrounded" by $\Gamma_n^*$. Let $C$ the (unique) constant sign cluster contained in $\mathrm{int}(\Gamma_n^*)$ that has sites next to $\Gamma_n^*$. Suppose that sites $x$ and $y$ in $C$ do not change sign at time $n+1$, then, at that time, they must belong to the same cluster $C'$. (This means that a cluster cannot split in two or more pieces under the effect of the dynamics.) The reason is that $x$ and $y$ are connected by an m-path $\Gamma$ at time $n$ because they are in the same cluster, and since they have not flipped between time $n$ and time $n+1$, Lemma 3.1 (or more accurately, the single time step analogue of Lemma 3.1) implies that the sites in $\Gamma$ have not flipped either, so that $x$ and $y$ are still connected at time $n+1$ and therefore belong to the same cluster.

If at least one site $x$ in $C$ does not change sign at time $n+1$, we say that $C$ has survived (and evolved into a new cluster $C'$ that contains $x$ at time $n+1$). From what we just said, the sites of $C$ that retain the same sign form a unique cluster $C'$. We call $C$ the parent cluster of $C'$ and the external boundary $\Gamma_n^* \in \mathcal{F}_\delta^n$ of $C$ the parent of the external boundary $\Gamma_{n+1}^* \in \mathcal{F}_\delta^{n+1}$ of $C'$ (note that $C'$ is a.s. finite – see Proposition 2.3). To prove that there is a one to one mapping between boundaries in $\mathcal{F}_\delta^{n+1}$ and those in $\mathcal{F}_\delta^n$, it remains to show that the parent boundary of each element of $\mathcal{F}_\delta^{n+1}$ is unique. (This means that clusters cannot merge under the effect of the dynamics.)

If this were not the case, then a cluster $C'$ could have two or more distinct parent clusters, $C_1, C_2, \ldots$ . Notice that each of the parent clusters at time $n$ is surrounded by a constant sign m-loop $\Gamma_i$, $i = 1, 2, \ldots$, which is stable. Suppose that $x_1 \in C_1$ and $x_2 \in C_2$ retain their sign at time $n+1$. Without loss of generality, we shall assume that this sign is plus. Assuming that $C_1$ and $C_2$ are both parents of $C'$, $x_1$ and $x_2$ should both belong to $C'$ at time $n+1$ and therefore be connected by a plus-path. But this contradicts the fact that, at time $n$, $x_1 \in \mathrm{int}(\Gamma_1)$ and $x_2 \in \mathrm{int}(\Gamma_2)$, that is, they belong to the interiors of two disjoint stable minus-loops. □

Notice that boundaries cannot be "created," but can "disappear," as complete clusters are "eaten" by the dynamics.

## 3.1 Proof of Theorem 1

Let us start, for simplicity, with the case of a single b-path. For any $\varepsilon > 0$, given a b-path $\Gamma_0^*$ at time 0, parametrized by some $\gamma(t)$, we will find a path $\Gamma_n^*$ at time $n$ with parametrization $\gamma'(t)$ such that, for $\delta$ small enough,

$$\sup_{t \in [0,1]} \mathrm{d}(\gamma(t), \gamma'(t)) \leq \varepsilon + 2\delta \tag{14}$$

and vice-versa (i.e., given $\Gamma_n^*$ and $\gamma'$, we need can find $\Gamma_0^*$ and $\gamma$ so that (14), in which the dependence on the scale factor $\delta$ has been suppressed, is valid). Later we will require that this holds simultaneously for all the curves in $\mathcal{F}_\delta^0$ and $\mathcal{F}_\delta^n$, as required by eq. (13).

Let $B^1(R)$ be the ball of radius $R$, $B^1(R) = \{u \in \mathbb{R}^2 : |u| \le R\}$ in the Euclidean metric, and $B^2(R) = \{u \in \mathbb{R}^2 : \mathrm{d}(u) \le R\}$ the ball of radius $R$ in the metric (10). For a given $\varepsilon > 0$, we divide $\mathbb{R}^2$ into two regions: $B^1(6/\varepsilon)$ and $\mathbb{R}^2 \setminus B^1(6/\varepsilon)$. We start by showing that, thanks to the choice of the metric (10), one only has to worry about curves (or polygonal paths) that intersect $B^1(6/\varepsilon)$. In fact, the distance between any two points $u, v \in \dot{\mathbb{R}}^2 \setminus B^1(6/\varepsilon)$ satisfies the following bound

$$\mathrm{d}(u,v) \le \mathrm{d}(u,\infty) + \mathrm{d}(v,\infty) \le 2\int_0^\infty [1 + (s + 6/\varepsilon)^2]^{-1}\, ds < \varepsilon/3. \tag{15}$$

Thus, given any curve in $\mathcal{F}_\delta^0$ contained completely in $\dot{\mathbb{R}}^2 \setminus B^1(6/\varepsilon)$, it can be approximated by any curve in $\mathcal{F}_\delta^n$ also contained in $\dot{\mathbb{R}}^2 \setminus B^1(6/\varepsilon)$, and vice-versa. The existence of such curves in $\mathcal{F}_\delta^0$ is clearly not a problem, since the region $\dot{\mathbb{R}}^2 \setminus B^1(6/\varepsilon)$ contains an infinite subset of $\delta\mathbb{T}$ and therefore there is zero probability that it doesn't contain any b-path at time zero. There is also zero probability that it contains no stable b-path at time zero, but any such b-path also belongs to $\mathcal{F}_\delta^n$.

Before we can proceed, we need the following lemma, which is a consequence of the the fact that at time zero we are dealing with a Bernoulli product measure. In this lemma (and elsewhere), the **diameter** $\mathrm{diam}(\cdot)$ of a subset of $\mathbb{R}^2$ is defined by using the Euclidean metric.

**Lemma 3.3.** *Let $\eta_0^*$ be any (deterministic) dual edge; then for some constant $c > 0$,*

$$\mu^0\left(\exists\, \Gamma^* \ni \eta_0^* : \mathrm{diam}(\Gamma^*) \ge M \text{ and } \Gamma^* \text{ does not contain at least one stable edge}\right) \le e^{-cM}. \tag{16}$$

*Proof.* To prove the lemma, we partition the hexagonal lattice into regions $Q_i$ as in Figure 5. We then do an algorithmic construction of $\Gamma^*$, starting from $\eta_0^*$, as a percolation exploration process, but with the additional rule that, when the exploration process hits the boundary of any $Q_i$ for the first time, all the hexagons in $Q_i$ are checked next (according to some deterministic order). From every entrance point of $Q_i$, there is a choice of the values of the spins of the outermost layer of $Q_i$ that forces $\Gamma^*$ to enter $Q_i$. Therefore, when $\Gamma^*$ hits $Q_i$, it always has a positive probability of entering the region.

We call $F_i$ the event that a (dual) stable edge is found inside $Q_i$, belonging to $\Gamma^*$. It is easy to see that such an event has positive probability, bounded away from zero by a constant that does not depend on how the exploration process enters the region $Q_i$. In fact, from any entrance point, there is clearly a choice of the values of the spins in $Q_i$ that forces $\Gamma^*$ to cut $Q_i$ in two symmetric parts, containing spins of opposite sign.

Now, if $\mathrm{diam}(\Gamma^*) \ge M$, then $\Gamma^*$ must clearly visit at least $O(M)$ different regions $Q_i$. The conclusion of the proof should now be clear (see, for example, [19]). □

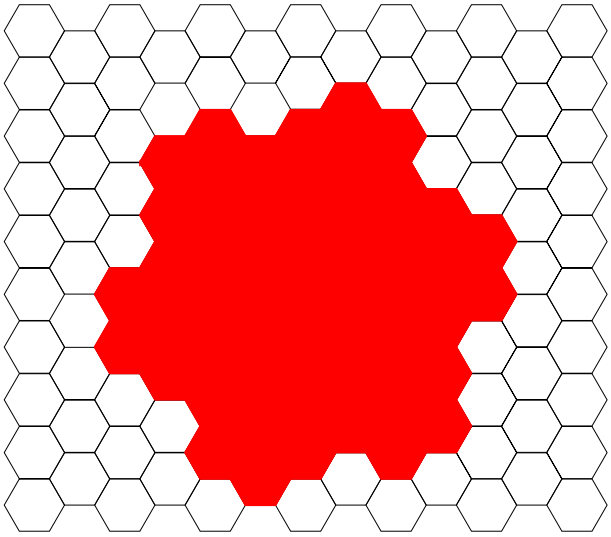

Figure 5: Elementary cell for the partition of $\mathbb{H}$ used in Lemma 3.3. Notice that the cell is made out of seven smaller cells, each of them formed by seven hexagons.

With this lemma, we can now proceed to the proof of the theorem. As explained before, we restrict attention to paths that intersect $B^1(6/\varepsilon)$. Given a b-path $\Gamma_0^* = (\eta_0^* = \eta_{\zeta_0,\xi_0}^*, \dots, \eta_k^* = \eta_{\zeta_k,\xi_k}^*)$ in $\mathcal{F}_\delta^0$ with parametrization $\gamma(t)$, call $u_0$ the point in $\mathbb{R}^2$ where the first (dual) edge $\eta_0^*$ begins. The following algorithmic construction produces a sequence $u_0, \dots, u_N$ of points in $\Gamma_0^*$.

1. Start with $u_0$.

2. Once $u_0, \dots, u_i$ have been constructed, if $u_i \in B^1(6/\varepsilon)$ take the ball $B_{u_i}^1(\varepsilon/3)$ centered at $u_i$ and of radius $\varepsilon/3$ and let $u_{i+1}$ be the first intersection of $\Gamma_0^* \setminus \Gamma_0^*(u_0, u_i)$ with $\partial B_{u_i}^1(\varepsilon/3)$, if $u_i \notin B^1(6/\varepsilon)$ take the ball $B_{u_i}^2(\varepsilon/3)$ centered at $u_i$ and of radius $\varepsilon/3$ and let $u_{i+1}$ be the first intersection of $\Gamma_0^* \setminus \Gamma_0^*(u_0, u_i)$ with $\partial B_{u_i}^2(\varepsilon/3)$.

3. Terminate when there is no next $u_i$.

During the construction of the sequence $u_0, \dots, u_N$, $\Gamma_0^*$ is split in $N+1$ pieces, the first $N$ having diameter at least $\varepsilon/3$. The construction also produces a sequence of balls $B_{u_0}^{j_0}(\varepsilon/3), \dots, B_{u_N}^{j_N}(\varepsilon/3)$, with $j_i = 1$ or 2. Notice that no two successive $u_i$'s can lie outside of $B^1(6/\varepsilon)$. In fact, if for some $i$, $u_i$ lies outside of $B^1(6/\varepsilon)$, $u_{i+1}$ belongs to $\partial B_{u_i}^2(\varepsilon/3)$, which is contained inside $B^1(6/\varepsilon)$, due to the choice of the metric. Each $u_i$ contained in $B^1(6/\varepsilon)$ lies on an edge of $\delta\mathbb{H}$, but no more than one $u_i$ can lie on the same edge since $\Gamma_0^*$ is self-avoiding and cannot use the same edge or site more than once. Also, the number of $u_i$'s lying outside of $B^1(6/\varepsilon)$ cannot be larger than (one more than) the number of the $u_i$'s lying inside $B^1(6/\varepsilon)$. Therefore, $N \leq const \times (\varepsilon\delta)^{-2}$.

For any two successive balls, $B_{u_i}^{j_i}(\varepsilon/3)$ and $B_{u_{i+1}}^{j_{i+1}}(\varepsilon/3)$, let $O_i = B_{u_i}^{j_i}(\varepsilon/3 + \delta) \cup B_{u_{i+1}}^{j_{i+1}}(\varepsilon/3 + \delta)$. Now assume that there exists a sequence $\bar{\eta}_0^*, \dots \bar{\eta}_{N-1}^*$ of stable (dual)

edges of $\Gamma_0^*$, with $\bar{\eta}_i^*$ contained in $\Gamma_0^*(u_i, u_{i+1})$. $\Gamma_0^*(\bar{\eta}_i^*, \bar{\eta}_{i+1}^*)$ is contained in $O_i$ (for fixed $\varepsilon$ and small enough $\delta$). Also contained in $O_i$ are the two paths (i.e., paths in $\delta\mathbb{T}$ which may be thought as sequences of hexagons) whose hexagons are next to $\Gamma_0^*(\bar{\eta}_i^*, \bar{\eta}_{i+1}^*)$, one on each side. From those two paths one can extract two subsets that are m-paths which are stable since the first and last hexagons of each one of them is stable (such hexagons must be stable since they are next to $\bar{\eta}_i^*$ and $\bar{\eta}_{i+1}^*$). The two m-paths so constructed constitute a "barrier" that limits the movements of the boundary, so that $\Gamma_n^*(\bar{\eta}_i^*, \bar{\eta}_{i+1}^*)$ is in fact confined to lie within those two m-paths and thus within $O_i$. To parametrize $\Gamma_n^*$, we use any parametrization $\gamma'(t)$ such that $\gamma'(t) = \gamma(t)$ whenever $\gamma(t) \in \bar{\eta}_i^*$. Using this parametrization and the previous fact, it is clear that the distance between $\Gamma_0^*(\bar{\eta}_i^*, \bar{\eta}_{i+1}^*)$ and $\Gamma_n^*(\bar{\eta}_i^*, \bar{\eta}_{i+1}^*)$ does not exceed $\varepsilon + 2\delta$, the diameter of $O_i$. Therefore, conditioning on the existence of the above sequence $\bar{\eta}_0^*, \ldots, \bar{\eta}_{N-1}^*$ of stable (dual) edges of $\Gamma_0^*$, we can conclude that

$$\sup_{t\in[0,1]} \mathrm{d}(\gamma(t), \gamma'(t)) \leq \varepsilon + 2\delta. \tag{17}$$

It remains to prove the existence of the sequence $\bar{\eta}_0^*, \ldots, \bar{\eta}_{N-1}^*$ of stable (dual) edges. To do that, let us call $A_i$ the event that $\Gamma_0^*(u_i, u_{i+1})$ does *not* contain at least one stable edge, and let $A = \cup_{i=0}^{N-1} A_i$ be the event that at least one of the first $N$ pieces of $\Gamma_0^*$ does not have any stable edge. Then, considering that the total number of edges contained in $B^1(6/\varepsilon)$ is bounded by $const \times (\varepsilon\delta)^{-2}$ and using Lemma 3.3, we have

$$\mu_\delta^0(A) \leq (\varepsilon\delta)^{-2} e^{-c'(\varepsilon/\delta)} \tag{18}$$

for some $c' > 0$. Equation (18) means that the probability of not finding at least one stable edge in each of the first $N$ pieces of $\Gamma_0^*$ is very small and goes to 0, for fixed $\varepsilon$, as $\delta \to 0$. This is enough to conclude that, with high probability (going to 1 as $\delta \to 0$), equation (17) holds.

This proves one direction of the claim, in the case of a single curve. To obtain the other direction, notice that a large b-path at time $n$ is part of a complete boundary $\Gamma_n^*$ which must come from a line of "ancestors" (see Lemma 3.2) that starts with some $\Gamma_0^*$ at time 0. Therefore, one can apply the above arguments to $\Gamma_0^*$, provided that the latter is large enough. Although the proof of this last fact is very simple, it is convenient to state it as a separate lemma.

**Lemma 3.4.** *Set $\delta = 1$ for simplicity; then for any boundary $\Gamma_n^*$ at time $n$, there is an ancestor $\Gamma_0^*$, with $diam(\Gamma_0^*) \geq diam(\Gamma_n^*) - 1$.*

*Proof.* The existence of an ancestor $\Gamma_0^*$ comes from Lemma 3.2, so we just have to show that $\mathrm{diam}(\Gamma_0^*) \geq \mathrm{diam}(\Gamma_n^*) - 1$. $\Gamma_0^*$ is surrounded by a connected set of hexagons that touch $\Gamma_0^*$ and whose spins are all the same (this is the "external boundary" of the set of hexagons that are in the interior of $\Gamma_0^*$). From this set, one can extract an m-path of constant sign whose diameter is bounded above by $\mathrm{diam}(\Gamma_0^*) + 1$. Since such a constant sign m-path is stable for the dynamics, $\Gamma_n^*$ must lie within its interior. This concludes the

proof. □

At this point, we need to show that the above argument can be repeated and the construction done simultaneously for all curves in $\mathcal{F}_\delta^0$ and $\mathcal{F}_\delta^n$ (for each $n$). First of all notice that, for a fixed $\varepsilon$, any b-path $\Gamma^*$ of diameter less than $\varepsilon/2$ can be approximated by a closest stable edge, provided that one is found within the ball of radius $\varepsilon/2$ that contains the $\Gamma^*$, with the probability of this last event clearly going to 1 as $\delta \to 0$, when we restrict attention to $B^1(6/\varepsilon)$. For a b-path outside $B^1(6/\varepsilon)$, we already noticed that it can be approximated by any other b-path also outside $B^1(6/\varepsilon)$. As for the remaining b-paths, notice that the total number of boundaries that intersect the ball $B^1(6/\varepsilon)$ cannot exceed $const \times (\varepsilon\delta)^{-2}$ (in fact, the total number of pieces in which the boundaries that intersect $B^1(6/\varepsilon)$ are divided cannot exceed $const \times (\varepsilon\delta)^{-2}$). So, we can carry out the above construction simultaneously for all the boundaries that touch $B^1(6/\varepsilon)$, having to deal with at most $const \times (\varepsilon\delta)^{-2}$ segments of b-paths of diameter of order at least $\varepsilon$. Therefore, letting $Y_\delta^n = \mathrm{dist}(\mathcal{F}_\delta^0, \mathcal{F}_\delta^n)$, we can apply once again Lemma 3.3 and conclude that

$$\mu^0(Y_\delta^n > \varepsilon) \leq (\varepsilon\delta)^{-2} e^{-c''(\varepsilon/\delta)}. \tag{19}$$

To show that $Y_\delta^n \to 0$ as $\delta \to 0$ $\mu^0$-almost surely and thus conclude the proof, it suffices to show that, $\forall \varepsilon > 0$, $\mu^0(\limsup_{\delta\to 0} Y_\delta^n > \varepsilon) = 0$. To that end, first take a sequence $\delta_k = 1/2^k$ and notice that

$$\sum_{k=0}^{\infty} \mu^0(Y_{\delta_k}^n > \varepsilon) \leq \sum_{k=0}^{\infty} \frac{4^k}{\varepsilon^2} e^{-c''2^k\varepsilon} < \infty, \tag{20}$$

where we have made use of (19). Equation (20) implies that we can apply the Borel-Cantelli lemma and deduce that $\mu^0(\limsup_{k\to\infty} Y_{\delta_k}^n > \varepsilon) = 0$, $\forall \varepsilon > 0$. In order to handle the values of $\delta$ not in the sequence $\delta_k$, that is for those $\delta$ such that $\delta_{k+1} < \delta < \delta_k$ for some $k$, we use the following double bound, valid for any $0 < \alpha < 1$,

$$\alpha \mathrm{d}(u, v) \leq \mathrm{d}(\alpha u, \alpha v) \leq \frac{1}{\alpha} \mathrm{d}(u, v), \tag{21}$$

which implies that $\alpha Y_{\delta_k}^n \leq Y_{\alpha\delta_k}^n \leq \frac{1}{\alpha} Y_{\delta_k}^n$. The two bounds in equation (21) come from writing $\mathrm{d}(\alpha u, \alpha v)$ as $\mathrm{d}(\alpha u, \alpha v) = \inf_{\phi'} \int (1 + |\phi'|^2)^{-1}\, ds' = \alpha \inf_{\phi} \int (1 + \alpha^2 |\phi|^2)^{-1}\, ds$, where $\phi'(s')$ are smooth curves joining $\alpha u$ with $\alpha v$, while $\phi(s)$ are smooth curves joining $u$ with $v$.

The proof of the theorem is now complete. □

## 3.2 Proof of Corollary 2.1

The Corollary is an immediate consequence of Theorem 1 and of the following general fact, of which we include the proof for completeness.

**Lemma 3.5.** *If $\{X_\delta\}, \{Y_\delta\}$ (for $\delta > 0$), and $X$ are random variables taking values in a complete, separable metric space $S$ (whose $\sigma$-algebra is the Borel algebra) with $\{X_\delta\}$ and $\{Y_\delta\}$ all defined on the same probability space, then if $X_\delta$ converges in distribution to $X$ and the metric distance between $X_\delta$ and $Y_\delta$ tends to zero almost surely as $\delta \to 0$, $Y_\delta$ also converges in distribution to $X$.*

*Proof.* Since $X_\delta$ converges to $X$ in distribution, the family $\{X_\delta\}$ is relatively compact and therefore tight by an application of Prohorov's Theorem (using the fact that $S$ is a complete, separable metric space – see, e.g., [7]). Then, for any bounded, continuous, real function $f$ on $S$, and for any $\varepsilon > 0$, there exists a compact set $K$ such that $\int |f(X_\delta)| I_{\{X_\delta \notin K\}} dP < \varepsilon$ and $\int |f(Y_\delta)| I_{\{X_\delta \notin K\}} dP < \varepsilon$ for all $\delta$, where $I_{\{\cdot\}}$ is the indicator function and $P$ the probability measure of the probability space of $\{X_\delta\}$ and $\{Y_\delta\}$. Thus, for small enough $\delta$,

$$\left| \int f(X_\delta) dP - \int f(Y_\delta) dP \right| < \int |f(X_\delta) - f(Y_\delta)| I_{\{X_\delta \in K\}} dP + 2\varepsilon < 3\varepsilon, \tag{22}$$

where in the last inequality we use the uniform continuity of $f$ when restricted to the compact set $K$ and the fact that the metric distance between $X_\delta$ and $Y_\delta$ goes to 0 as $\delta \to 0$. □

To conclude the proof of the Corollary, it is enough to apply Lemma 3.5 to $\{\mu_\delta^0\}_\delta$, $\{\mu_\delta^n\}_\delta$, $\mu_{sl}$ (or, to be more precise, to the random variables of which those are the distributions), for each $n \in [1, \infty]$, where $\mu_{sl}$ is the unique scaling limit of critical site percolation on the triangular lattice. □

# 4 Dependent site percolation models on the hexagonal and triangular lattice

The model that we have presented and discussed in Section 2 has been chosen as a sort of paradigm, but is not the only one for which such results can be proved. In fact, it is not the original model for which such results were obtained.

In this section we describe some percolation models on the *hexagonal* lattice and prove that they have the same scaling limit as critical (independent) site percolation on the *triangular* lattice. None are independent percolation models, but nonetheless, they represent explicit examples of critical percolation models on different lattices with the same scaling limit. Besides, the construction of the models on the hexagonal lattice can be seen as a simple and natural way of producing percolation models for which all the sites of the external (site) boundary of any constant sign cluster $C$ belong to a unique cluster $C'$ of opposite sign. In other words, this implies that the the boundaries between clusters of opposite sign form a nested collection of loops, a property that site percolation on the triangular lattice possesses automatically because of the *self-matching* property of $\mathbb{T}$ (which is crucial in Smirnov's proof of the existence and uniqueness of the scaling limit of crossing probabilities and Cardy's formula).

## 4.1 The models

The percolation models that we briefly describe here can be constructed by means of a natural *zero-temperature Glauber dynamics* which is the zero-temperature case of *Domany's stochastic Ising ferromagnet* on the hexagonal lattice [18]. The cellular automaton (i.e., Domany's stochastic Ising ferromagnet at zero temperature) that gives rise to those percolation models can also be realized on the triangular lattice with flips when a site disagrees with six, five and sometimes four of its six neighbors. The initial state $\sigma^0$ consists of an assignment of $-1$ or $+1$ with equal probability to each site of the hexagonal or triangular lattice (depending on which version of the cellular automaton we are referring to). In the first version, $\mathbb{H}$, as a bipartite graph, is partitioned into two subsets $\mathcal{A}$ and $\mathcal{B}$ which are alternately updated so that each $\sigma_x$ is forced to agree with a majority of its three neighbors (which are in the other subset). In the second version, all sites are updated simultaneously according to a rule based on a deterministic pairing of the six neighbors of every site into three pairs. The rule is that $\sigma_x$ flips if and only if it disagrees with both sites in two or more of its three neighbor pairs; thus there is (resp., is not) a flip if the number $D_x$ of disagreeing neighbors is $\geq 5$ (resp., $\leq 3$) and there is also a flip for some cases of $D_x = 4$. These percolation models on $\mathbb{H}$ and $\mathbb{T}$ are investigated in [15], where Cardy's formula for rectangular crossing probabilities is proved to hold in the scaling limit.

The discrete time cellular automaton corresponding to the zero-temperature case of Domany's stochastic Ising ferromagnet on the hexagonal lattice can be considered as a simplified version of a continuous time Markov process where an independent (rate 1) Poisson clock is assigned to each site $x \in \mathbb{H}$, and the spin at site $x$ is updated (with the same rule as in our discrete time dynamics) when the corresponding clock rings. (In particular, they have the same stable configurations – see Figure 6.) The percolation properties of the final state $\sigma^\infty$ of that process were studied, both rigorously and numerically, in [27]; the results there (about critical exponents rather than the continuum scaling limit) strongly suggest that that dependent percolation model is also in the same universality class as independent percolation. Similar stochastic processes on different types of lattices have been studied in various papers. See, for example, [10, 20, 22, 37, 38, 39, 40] for models on $\mathbb{Z}^d$ and [26] for a model on the homogeneous tree of degree three. Such models are also discussed extensively in the physics literature, usually on $\mathbb{Z}^d$ (see, for example, [18] and [35]). Numerical simulations have been done by Nienhius [41] and rigorous results for both the continuous and discrete dynamics have been obtained in [14], including a detailed analysis of the discrete time (synchronous) case.

Let us now describe in more detail the two deterministic cellular automata (on $\mathbb{H}$ and $\mathbb{T}$). Later, we will prove the equivalence of the percolation models generated by those cellular automata.

**Zero-temperature Domany model**

Consider the homogeneous ferromagnet on the hexagonal lattice $\mathbb{H}$ with states denoted

by $\sigma = \{\sigma_x\}_{x\in\mathbb{H}}$, $\sigma_x = \pm 1$, and with (formal) Hamiltonian

$$\mathcal{H}(\sigma) = -\sum_{\langle x,y\rangle} \sigma_x\sigma_y, \tag{23}$$

where $\sum_{\langle x,y\rangle}$ denotes the sum over all pairs of neighbor sites, each pair counted once. We write $\mathcal{N}^{\mathbb{H}}(x)$ for the set of three neighbors of $x$, and indicate with

$$\Delta_x\mathcal{H}(\sigma) = 2\sum_{y\in\mathcal{N}^{\mathbb{H}}(x)} \sigma_x\sigma_y \tag{24}$$

the change in the Hamiltonian when the spin $\sigma_x$ at site $x$ is flipped (i.e., changes sign).

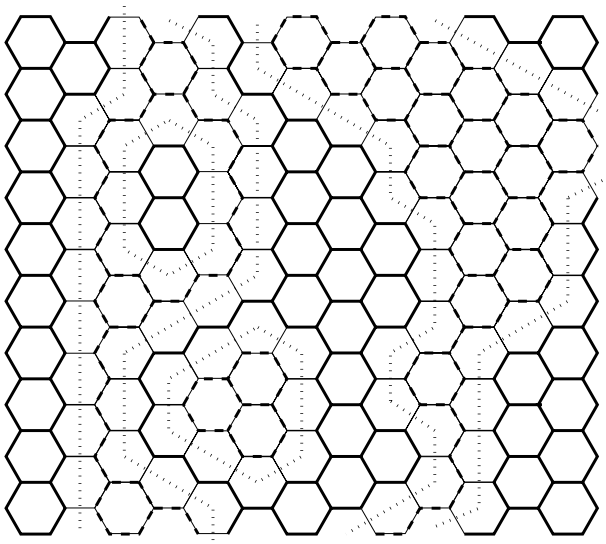

Figure 6: Example of a (local) stable configuration for the zero-temperature Domany dynamics. Heavy lines on edges of $\mathbb{H}$ connect, say, plus spins, while heavy broken lines connect minus spins. The dotted lines drawn on edges of the dual lattice are the perpendicular bisectors of unsatisfied edges, indicating the boundaries between plus and minus clusters. Every spin has at least two neighbors of the same sign, since only loops and barbells are stable under the effect of the dynamics.

The hexagonal lattice $\mathbb{H}$ is partitioned into two subsets $\mathcal{A}$ and $\mathcal{B}$ in such a way that all three neighbors of a site $x$ in $\mathcal{A}$ (resp., $\mathcal{B}$) are in $\mathcal{B}$ (resp., $\mathcal{A}$). By joining two sites of $\mathcal{A}$ whenever they are next-nearest neighbors in the hexagonal lattice (two steps away from each other), we get a triangular lattice (the same with $\mathcal{B}$) (see figure 7). The synchronous dynamics is such that all the sites in the sublattice $\mathcal{A}$ (resp., $\mathcal{B}$) are updated simultaneously.

We now define the discrete time Markov process $\sigma^n$, $n \in \mathbb{N}$, with state space $\mathcal{S}_{\mathbb{H}} = \{-1, +1\}^{\mathbb{H}}$, which is the zero temperature limit of a model of Domany [18], as follows:

- The initial state $\sigma^0$ is chosen from a symmetric Bernoulli product measure.
- At odd times $n = 1, 3, \ldots$, the spins in the sublattice $\mathcal{A}$ are updated according to the following rule: $\sigma_x$, $x \in \mathcal{A}$, is flipped if and only if $\Delta_x \mathcal{H}(\sigma) < 0$.
- At even times $n = 2, 4, \ldots$, the spins in the sublattice $\mathcal{B}$ are updated according to the same rule as for those of the sublattice $\mathcal{A}$.

**Cellular automaton on $\mathbb{T}$**
We define here a deterministic cellular automaton Q on the triangular lattice $\mathbb{T}$, with random initial state chosen by assigning value $+1$ or $-1$ independently, with equal probability, to each site of $\mathbb{T}$.

Given some site $\bar{x} \in \mathbb{T}$, group its six $\mathbb{T}$-neighbors $y$ in three disjoint pairs $\{y_1^{\bar{x}}, y_2^{\bar{x}}\}$, $\{y_3^{\bar{x}}, y_4^{\bar{x}}\}$, $\{y_5^{\bar{x}}, y_6^{\bar{x}}\}$, so that $y_1^{\bar{x}}$ and $y_2^{\bar{x}}$ are $\mathbb{T}$-neighbors, and so on for the other two pairs. Translate this construction to all sites $x \in \mathbb{T}$, thus producing three pairs of sites $\{y_1^x, y_2^x\}$, $\{y_3^x, y_4^x\}$, $\{y_5^x, y_6^x\}$ associated to each site $x \in \mathbb{T}$. (Note that this construction does not need to specify how $\mathbb{T}$ is embedded in $\mathbb{R}^2$.) Site $x$ is updated at times $m = 1, 2, \ldots$ according to the following rule: the spin at site $x$ is changed from $\sigma_x$ to $-\sigma_x$ if and only if at least two of its pairs of neighbors have the same sign and this sign is $-\sigma_x$.

## 4.2 Equivalence between the models on $\mathbb{H}$ and $\mathbb{T}$

We show here how the models on the hexagonal and on the triangular lattice are related through a *star-triangle transformation*. More precisely, we will show that the dynamics on the triangular lattice $\mathbb{T}$ is equivalent to the alternating sublattice dynamics on the hexagonal lattice $\mathbb{H}$ when restricted to the sublattice $\mathcal{B}$ for even times $n = 2m$.

To see this, start with $\mathbb{T}$ and construct an hexagonal lattice $\mathbb{H}'$ by means of a star-triangle transformation (see, for example, p. 335 of [23]) such that a site is added at the center of each of the triangles $(x, y_1^x, y_2^x), (x, y_3^x, y_4^x)$, and $(x, y_5^x, y_6^x)$ (the sites $y_i^x$ are defined in the previous subsection). $\mathbb{H}'$ may be partitioned into two triangular sublattices $\mathcal{A}'$ and $\mathcal{B}'$ with $\mathcal{B}' = \mathbb{T}$. One can now see that the dynamics on $\mathbb{T}$ for $m = 1, 2, \ldots$ and the alternating sublattice dynamics on $\mathbb{H}'$ restricted to $\mathcal{B}'$ for even times $n = 2m$ are the same.

An immediate consequence of this equivalence between the two cellular automata is that the two families of percolation models that they produce are also equivalent in an obvious way through a star-triangle transformation. To be more precise, the percolation models defined on $\mathbb{T}$ by $Q$ for times $m = 1, 2, \ldots$ are the same as those defined on $\mathcal{B}$ by the zero-temperature Domany model for even times $n = 2m$.

## 4.3 Results for the zero-temperature Domany model

In this section we explain how the results obtained for the percolation models $\mu_\delta^n$ generated by the cellular automaton T are also valid for the percolation models defined by the zero-temperature Domany model. Because of the results of the previous section, we

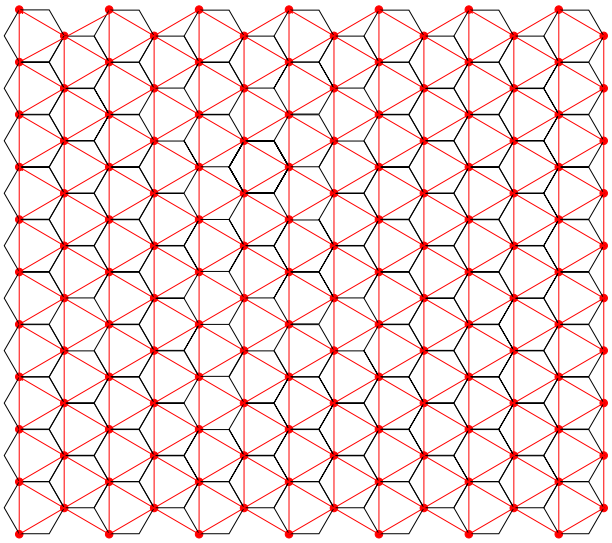

Figure 7: A star-triangle transformation.

can actually consider the percolation models $\tilde{\mu}_\delta^n$ on $\delta\mathbb{T}$ generated by Q, for which we have results analogous to Theorem 1 and Corollary 2.1. Results equivalent to Propositions 2.1, 2.2 and 2.3 are contained in [14]. The proof of the main theorem (i.e., the analogue of Theorem 1) is basically the same as for the models generated by T, so we just point out the differences. We follow here the setup and notation of [14], but give all the relevant definitions in order to make this paper self-consistent.

Let us consider a loop $\Gamma$ in the triangular sublattice $\mathcal{B}$, written as an ordered sequence of sites $(y_0, y_1, \ldots, y_k)$ with $k \geq 3$, which are distinct except that $y_k = y_0$. For $i = 1, \ldots, k$, let $\zeta_i$ be the unique site in $\mathcal{A}$ that is an $\mathbb{H}$-neighbor of both $y_{i-1}$ and $y_i$. We call $\Gamma$ an **s-loop** if $\zeta_1, \ldots, \zeta_k$ are all distinct. Similarly, a (site-self avoiding) path $(y_0, y_1, \ldots, y_k)$ in $\mathcal{B}$, between $y_0$ and $y_k$, is called an **s-path** if $\zeta_1, \ldots, \zeta_k$ are all distinct. Notice that any path in $\mathcal{B}$ between $y$ and $y'$ (seen as a collection of sites) contains an s-path between $y$ and $y'$. An s-loop of constant sign is stable for the dynamics since at the next update of $\mathcal{A}$ the presence of the constant sign s-loop in $\mathcal{B}$ will produce a stable loop of that sign in the hexagonal lattice. Similarly an s-path of constant sign between $y$ and $y'$ will be stable if $y$ and $y'$ are stable — e.g., if they each belong to an s-loop. A triangular loop $x_1, x_2, x_3 \in \mathcal{B}$ with a common $\mathbb{H}$-neighbor $\zeta \in \mathcal{A}$ is called a **star**; it is not an s-loop. A triangular loop in $\mathcal{B}$ that is not a star is an s-loop and will be called an **antistar**, while any loop in $\mathcal{B}$ that contains more than three sites contains an s-loop.

With these definitions, the proof of the main theorem for the zero-temperature Domany model is the same as that presented in Section 3 for our prototypical model, with the role of loops in the original proof played here by s-loops (in particular antistars), and that of m-paths by s-paths (see Section 3 below).

### 4.4 An amusing further example: totally synchronous dynamics on $\mathbb{H}$

The model that we consider here corresponds to the zero-temperature Glauber dynamics on the hexagonal lattice with *all* sites updated simultaneously at discrete times, *without* alternating between two subsets (contrary to the case of the zero-temperature Domany model), with initial configuration $\sigma^0$ chosen according to a symmetric Bernoulli product measure.

Let us partition $\mathbb{H}$ in two subsets $\mathcal{A}$ and $\mathcal{B}$ as before and define the family of percolation models $\{\bar{\mu}^m_{\mathcal{A}}, m = 0, 1, \dots\}$, where $\bar{\mu}^m_{\mathcal{A}}$ is the distribution of $\sigma^{2m}$ (at even times) restricted to the subset $\mathcal{A}$ (naturally endowed with a triangular lattice structure, so that $\bar{\mu}^0_{\mathcal{A}}$ is the distribution of critical site percolation).

The main difference consists in the fact that $\sigma^n$ does not fixate as $n \to \infty$ since there is a positive density of spins that flip infinitely many times. To see this, consider a loop $\Gamma$ in $\mathbb{H}$ containing an even number of sites and such that at time zero its spins are alternately plus and minus. At any time $n$, every spin in $\Gamma$ has two neighbors of opposite sign and will therefore flip at the next update. Thus, the spins in $\Gamma$ never stop flipping.

However, there is a simple observation that tremendously simplifies the analysis of this totally synchronous dynamics. Namely, that if we restrict attention to sublattice $\mathcal{A}$ at odd times $n = 1, 3, 5, \dots$ and sublattice $\mathcal{B}$ at even times $n = 0, 2, 4, \dots$, the dynamics is *identical* to the zero-temperature Domany dynamics discussed above (let us call this $\sigma^n_a$). On the other hand, if we instead observe $\mathcal{A}$ at even times and $\mathcal{B}$ at odd times, this is identical to an alternative zero-temperature Domany type dynamics $\sigma^n_b$ but with the first (and third and $\dots$) update on $\mathcal{B}$ rather than $\mathcal{A}$. Furthermore, $(\sigma^n_a)_{n=0}^{\infty}$ and $(\sigma^n_b)_{n=0}^{\infty}$ are completely independent of each other. We conclude that there are two distinct limits $\sigma^\infty_a$ and $\sigma^\infty_b$ (independent of each other) and that the scaling limit of $\sigma^n$ restricted to either $\mathcal{A}$ or $\mathcal{B}$ is the same as for independent critical percolation on $\mathbb{T}$. But it appears that for any $n$, $\sigma^n$ on all of $\mathbb{H}$ should be subcritical and thus have a trivial scaling limit.

# References


[1] M. Aizenman. The geometry of critical percolation and conformal invariance, in *StatPhys 19* (H. Balin ed.), World Scientific (1995).

[2] M. Aizenman. Scaling limit for the incipient spanning clusters, in *Mathematics of Multiscale Materials; the IMA Volumes in Mathematics and its Applications* (K. Golden, G. Grimmett, R. James, G. Milton, and P. Sen eds.), Springer (1998).

[3] M. Aizenman, A. Burchard. Holder regularity and dimension bounds for random curves. *Duke Math. J.* **99**, 419-453 (1999).

[4] M. Aizenman, A. Burchard, C. M. Newman, D. B. Wilson. Scaling Limits for Minimal and Random Spanning Trees in Two Dimensions. *Random Struct. Alg.* **15**, 319-367 (1999).

[5] A. A. Belavin, A. M. Polyakov, A. B. Zamolodchikov. Infinite conformal symmetry of critical fluctuations in two dimensions. *J. Stat. Phys.* **34**, 763-774 (1984).

[6] A. A. Belavin, A. M. Polyakov, A. B. Zamolodchikov. Infinite conformal symmetry in two-dimensional quantum field theory. *Nucl. Phys.* **B241**, 333-380 (1984).

[7] P. Billingsley. *Convergence of Probability Measures*. John Wiley & Sons, Inc., New York (1968).

[8] F. Camia. Scaling Limit and Critical Exponents for 2D Bootstrap Percolation. In preparation.

[9] F. Camia. Universality in Two-Dimensional Enhancement Percolation. In preparation.

[10] F. Camia, E. De Santis, C. M. Newman. Clusters and recurrence in the two-dimensional zero-temperature stochastic Ising model. *Ann. Appl. Probab.* **12**, 565-580 (2002).

[11] F. Camia, C. M. Newman. The Percolation Transition in the Zero-Temperature Domany Model. *J. Stat. Phys.*, to appear.

[12] F. Camia, C. M. Newman. Continuum Nonsimple Loops and 2D Critical Percolation. Preprint arXiv:math.PR/0308122.

[13] F. Camia, C. M. Newman. In preparation.

[14] F. Camia, C. M. Newman, V. Sidoravicius. Approach to fixation for zero-temperature stochastic Ising models on the hexagonal lattice. In *In and out of equilibrium: Probability with a Physics Flavor* (V. Sidoravicius ed.), Progress in Probability **51**, 163-183, Birkhäuser (2002).

[15] F. Camia, C. M. Newman, V. Sidoravicius. Cardy's Formula for some Dependent Percolation Models. *Bull. Brazilian Math. Soc.* **33**, 147-156 (2002).

[16] J. L. Cardy. Critical percolation in finite geometries. *J. Phys. A* **25**, L201-L206 (1992).

[17] J. Cardy. Lectures on Conformal Invariance and Percolation. Preprint arXiv:math-ph/0103018.

[18] E. Domany. Exact results for two- and three-dimensional Ising and Potts models. *Phys. Rev. Lett.* **52**, 871-874 (1984).

[19] L. R. Fontes, C. M. Newman. First passage percolation for random colorings of $\mathbb{Z}^d$. *Ann. Appl. Probab.* **3**, 746-762 (1993).

[20] L. R. Fontes, R. H. Schonmann, V. Sidoravicius. Stretched exponential fixation in stochastic Ising models at zero temperature. *Commun. Math. Phys.* **228**, 495-518 (2002).

[21] A. Gandolfi, M. Keane, L. Russo. On the uniqueness of the infinite occupied cluster in dependent two-dimensional site percolation. *Ann. Probab.* **16**, 1147-1157 (1988).

[22] A. Gandolfi, C. M. Newman, D. L. Stein. Zero-temperature dynamics of $\pm J$ spin glasses and related models. *Commun. Math. Phys.* **214**, 373-387 (2000).

[23] G. R. Grimmett. *Percolation*. Second edition. Springer, Berlin (1999).

[24] E. A. Guggenheim. The Principle of Corresponding States. *J. Chem. Phys.* **13**, 253-261 (1945).

[25] T. E. Harris. A correlation inequality for Markov processes in partially ordered state spaces. *Ann. Probab.* **5**, 451-454 (1977).

[26] C. D. Howard. Zero-temperature Ising spin dynamics on the homogeneous tree of degree three. *J. Appl. Probab.* **37**, 736-747 (2000).

[27] C. D. Howard, C. M. Newman. The percolation transition for the zero-temperature stochastic Ising model on the hexagonal lattice. *J. Stat. Phys.* **111**, 57-72 (2003).

[28] G. Lawler, O. Schramm, W. Werner. Values of Brownian intersection exponents I: Half-plane exponents. *Acta Math.* **187**, 237-273 (2001).

[29] G. Lawler, O. Schramm, W. Werner. Values of Brownian intersection exponents II: Plane exponents. *Acta Math.* **187**, 275-308 (2001).

[30] G. Lawler, O. Schramm, W. Werner. Values of Brownian intersection exponents III: Two-sided exponents. *Ann. Inst. Henri Poincaré* **38**, 109-123 (2002).

[31] G. Lawler, O. Schramm, W. Werner. Analyticity of intersection exponents for planar Brownian motion. *Acta Math.* **189**, 179-201 (2002).

[32] G. Lawler, O. Schramm, W. Werner. One arm exponents for critical 2D percolation. *Electronic J. Probab.* **7**, paper no. 2 (2002).

[33] G. Lawler, O. Schramm, W. Werner. Conformal invariance of planar loop-erased random walk and uniform spanning trees. *Ann. Probab.*, to appear. Preprint arXiv:math.PR/0112234 (2003).

[34] G. Lawler, O. Schramm, W. Werner. Conformal restriction: the chordal case. *J. Amer Math. Soc.*, to appear. Preprint arXiv:math.PR/0209343 (2003).

[35] J. L. Lebowitz, C. Maes, E. R. Speer. Statistical mechanics of probabilistic cellular automata. *J. Stat. Phys.* **59**, 117-170 (1990).

[36] T. M. Liggett. *Interacting Particle Systems*. Springer, New York (1985).

[37] S. Nanda, C. M. Newman, D. L. Stein. Dynamics of Ising spin systems at zero temperature. In *On Dobrushin's Way (from Probability Theory to Statistical Mechanics)* (R. Minlos, S. Shlosman and Y. Suhov, eds.). AMS, Providence (2000).

[38] C. M. Newman, D. L. Stein. Blocking and persistence in zero-temperature dynamics of homogeneous and disordered Ising models. *Phys. Rev. Lett.* **82**, 3944-3947 (1999).

[39] C. M. Newman, D. L. Stein. Equilibrium pure states and nonequilibrium chaos. *J. Stat. Phys.* **94**, 709-722 (1999).

[40] C. M. Newman, D. L. Stein. Zero-temperature dynamics of Ising spin systems following a deep quench: results and open problems. *Physica A* **279**, 156-168 (2000).

[41] B. Nienhuis. Private communication (2001).

[42] L. Onsager (1944). Crystal Statistics I. A two-dimensional model with an order-disorder transition. *Phys. Rev.* **65**, 117-149 (1944).

[43] H. Pinson, T. Spencer. Universality in the 2D Critical Ising Model. Preprint.

[44] L. Russo. A note on percolation. *Z. Wahrsch. Verw. Gebiete* **43**, 39-48 (1987).

[45] O. Schramm. Scaling limits of loop-erased random walks and uniform spanning trees. *Israel J. Math.* **118**, 221-228 (2001).

[46] O. Schramm. A percolation formula, *Elect. Comm. Probab.* **6**, 115-120 (2001).

[47] S. Smirnov. Critical percolation in the plane. I. Conformal invariance and Cardy's formula. II. Continuum scaling limit. (long version of [48], dated Nov. 15, 2001). Available at http://www.math.kth.se/∼stas/papers/index.html.

[48] S. Smirnov. Critical percolation in the plane: Conformal invariance, Cardy's formula, scaling limits. *C. R. Acad. Sci. Paris* **333**, 239-244 (2001).

[49] S. Smirnov, W. Werner (2001). Critical exponents for two-dimensional percolation. *Math. Rev. Lett.* **8**, 729-744 (2001).

[50] A. D. Sokal. Lecture notes, unpublished.

[51] J. D. van der Waals. Doctoral thesis (1873) and *Die Continuität des Gasförmingen und Flüssigen Zustandes*. Verlag von J.A. Barth, Leipzig (1899).

[52] P.-E. Weiss. L'hypothèse du champ moléculaire et la proprieté ferromagnétique. *J. de Phys.*, Series 4, Vol. **6**, 661-690 (1907).